Development 127, 4217-4226 (2000)
Printed in Great Britain © The Company of Biologists Limited 2000
DEV8755

Fork head prevents apoptosis and promotes cell shape change during formation of the *Drosophila* salivary glands

Monn Monn Myat and Deborah J. Andrew*

Department of Cell Biology and Anatomy, The Johns Hopkins University School of Medicine, 725 N. Wolfe Street, Baltimore, MD 21205-2196, USA
*Author for correspondence (e-mail: dandrew@jhmi.edu)

Accepted 13 July; published on WWW 7 September 2000

SUMMARY

The secretory tubes of the *Drosophila* salivary glands are formed by the regulated, sequential internalization of the primordia. Secretory cell invagination occurs by a change in cell shape that includes basal nuclear migration and apical membrane constriction. In embryos mutant for *fork head* (*fkh*), which encodes a transcription factor homologous to mammalian hepatocyte nuclear factor 3β (HNF-3β), the secretory primordia are not internalized and secretory tubes do not form. Here, we show that secretory cells of *fkh* mutant embryos undergo extensive apoptotic cell death following the elevated expression of the apoptotic activator genes, *reaper* and *head involution defective*. We rescue the secretory cell death in the *fkh* mutants and show that the rescued cells still do not invaginate. The rescued *fkh* secretory cells undergo basal nuclear migration in the same spatial and temporal pattern as in wild-type secretory cells, but do not constrict their apical surface membranes. Our findings suggest at least two roles for *fkh* in formation of the embryonic salivary glands: an early role in promoting survival of the secretory cells, and a later role in secretory cell invagination, specifically in the constriction of the apical surface membrane.

Key words: Apoptosis, *Drosophila melanogaster*, *fork head*, Morphogenesis, Salivary gland

INTRODUCTION

During embryonic development of many organisms, the movement and folding of epithelial layers give rise to a variety of tissues and organs. Epithelial invagination is a morphogenetic movement by which the epithelium folds inward through a process involving individual cell shape changes (reviewed by Ettensohn, 1985; Fristrom, 1988). Several general models have been proposed to explain how an epithelium invaginates. In the apical constriction model, nuclei migrate to a more basal position and the apical membranes constrict, thus turning a columnar cell into a wedge-shaped one. Changes in the underlying microfilament and microtubule systems are thought to drive this change in cell shape (reviewed by Ettensohn, 1985; Messier, 1978). In the second model for invagination, changes in cell-cell adhesion are proposed to drive internalization (Gustafson and Wolpert, 1962; Nardi, 1981; Mittenthal and Mazo, 1983). If an increase in adhesion between cells of an invaginating epithelium results in increased cell height while leaving the basal surface adherent to the substratum, the apical surface area would decrease, causing the epithelium to fold inward. During invagination of the mesodermal primordia in *Drosophila* embryos, changes in the location, size and morphology of the cadherin- and catenin-based adhesion junctions are associated with changes in the shape and internalization of the cells (Oda et al., 1998), supporting the cell-cell adhesion model for invagination. In the third model, changes in the extracellular matrix (ECM) are proposed to drive invagination (Lane et al., 1993). In gastrulating sea urchin embryos, invaginating cells are proposed to deposit a new hygroscopic layer of ECM between their apical surfaces and the older less hygroscopic layer. The new, more hygroscopic layer of ECM swells and increases in surface area due to its greater hydration, thus driving the bilayered ECM and underlying epithelial sheet to bend inward.

Recent studies on epithelial invagination in genetically manipulatable organisms, such as *C. elegans* and *D. melanogaster*, have begun to identify mutations that affect invagination. A screen for mutations affecting vulval invagination in *C. elegans* identified the *squashed vulva* (*sqv*) genes that most likely encode components of a conserved glycosylation pathway (Herman et al., 1999; Herman and Horvitz, 1999). In *sqv* mutants, the vulval invagination partially collapses, resulting in a reduced invagination space (Herman et al., 1999). The *sqv* genes are proposed to establish and/or maintain the rigidity of the invaginating vulval epithelium. The collapsed phenotype could be either due to defects in adhesion between the invaginating cells or, perhaps more likely, due to defects in the rigidity of the ECM that lines the invaginating space.

In the gastrulating *Drosophila* embryo, epithelial invagination occurs during the internalization of the

mesodermal primordium, and the anterior and posterior midgut primordia (reviewed by Leptin, 1999). Genetic studies in *Drosophila* identified two signaling molecules that regulate internalization of these tissues: Folded gastrulation (FOG), a putative secreted molecule, and Concertina (CTA), a putative Gα-like protein (Parks and Wieschaus, 1991; Costa et al., 1994). In *fog* mutant embryos, the mesodermal primordium is internalized, although in an uncoordinated manner, and the posterior midgut primordium completely fails to internalize (Parks and Wieschaus, 1991; Sweeton et al., 1991). The FOG signal is transduced via an unknown receptor to CTA, which then relays the signal to the cytoskeleton, causing cell shape change (Costa et al., 1994). The FOG/CTA signal most likely affects the actin cytoskeleton by activating RhoGEF2, which acts as a GTP exchange factor for a member of the Rho family of GTPases (Barrett et al., 1997; Hacker and Perrimon, 1998). Hyperactivation of the FOG/CTA signaling pathway causes ectopic apical constriction and cell shape change (Morize et al., 1998).

Internalization of the *Drosophila* salivary gland also occurs by invagination through changes in cell shape (Myat and Andrew, 2000). The secretory tubes arise from two placodes of epithelial cells at the ventral surface (reviewed by Andrew et al., 2000). The columnar placode cells become wedge-shaped through the constriction of their apical surface membranes and the coordinated migration of their nuclei to the basal domain (Myat and Andrew, 2000). The cell shape changes and subsequent invagination in the secretory primordia are both regulated events. In embryos mutant for the transcription factor, Huckebein (HKB), secretory cells become wedge-shaped and invaginate, but are not internalized in the same order as in wild-type embryos. As a consequence, the secretory tubes are round and remain closely associated with the anterior embryo surface, instead of being cylindrical and associating with the lateral body wall as in wild-type embryos. *hkb* expression in the secretory primordia presages the order in which cells change shape and invaginate, suggesting that *hkb* may play an instructive role in determining the order of invagination.

fork head (*fkh*), like *hkb*, is among the earliest genes to be expressed in the secretory primordia. *fkh* encodes a transcription factor of the winged-helix family, and is homologous to mammalian HNF3β (Weigel et al., 1989b). In *fkh* mutant embryos, salivary glands do not form, even though the secretory primordia are established (Weigel et al., 1989a). In this report, we show that *fkh* has a dual role in salivary gland formation, one in secretory cell survival and a second in cell shape change, specifically in the constriction of the apical surface membrane.

MATERIALS AND METHODS

Drosophila strains

The wild-type flies used in all experiments were Oregon R. The fkh^6 allele and the *Df(3L)H99* strain are described in Flybase (1999). The *UAS-rpr*, *UAS-hid*, *UAS-grim* flies (provided by H. Steller, Massachusetts Institute of Technology) and *UAS-rpr*; *UAS-hid* flies (provided by J. Nambu, University of Massachusetts) were crossed to *fkh*-GAL4 flies (Henderson and Andrew, 2000) to induce apoptosis in the salivary glands. The expression profile of GAL4 in *fkh*-GAL4 embryos was detected by antibody staining for GAL4 (Santa Cruz Biotechnologies, Santa Cruz). *Df(3L)H99* was recombined onto a fkh^6 mutant chromosome; the genotype of the recombinant fkh^6 *Df(3L)H99* chromosome was confirmed by whole-mount in situ hybridizations with *rpr* and *hid* antisense RNA probes, which did not detect transcript in the homozygotes (see below).

Antibody staining and whole-mount in situ hybridizations

The rat dCREB-A antiserum (Andrew et al., 1997) was used at a dilution of 1:5000. The rat CRQ antiserum (Franc et al., 1999) was used at a dilution of 1:1000. The rat PASILLA (PS) antiserum (Seshaiah, 2000) was used at a dilution of 1:5000. The mouse monoclonal β-galactosidase (β-gal) antibody (Promega; Madison, WI) was used at a dilution of 1:5000. Embryo fixation and staining were performed as described by Reuter et al. (1990). Embryos homozygous for *fkh*, *fkh H99* or *H99* were unambiguously identified by the absence of staining for β-gal, which detects the expression of the *Ubx-lacZ* insert on the TM6B balancer chromosome. Immunostained embryos were mounted in methylsalicylate (Sigma, Missouri, IL) and visualized and photographed on a Zeiss Axiophot microscope (Carl Zeiss, Thornwood, NY) using Nomarski optics and Kodak print film (Eastman Kodak, Rochester, NY). Embryonic mRNA was detected by whole-mount in situ hybridization as described by Lehmann and Tautz (1994). *rpr* and *hid* cDNAs (provided by E. Baehracke), and a *grim* cDNA (provided by J. Abrams) were used to make antisense riboprobes. Embryos were mounted in 70% glycerol and visualized and photographed as described above for antibody-stained embryos.

Thick sections of Epon-embedded embryos

Embryos processed for antibody staining with α-dCREB-A and α-β-gal were embedded in Epon (Eponate Kit™, Ted Pella, Reading, CA) as previously described (Myat and Andrew, 2000). One μm thick sections, obtained on a Reichart-Jung Ultracut E (Leica Inc.) microtome, were counter-stained with 1% Toluidine Blue and 1% sodium borate (Sigma, Missouri, IL). Stained sections were mounted in Permount (Fisher Scientific; Pittsburgh, PA) and viewed and photographed as described above for antibody-stained embryos.

Transmission electron microscopy

Embryos were processed for TEM by first dechorionating them in 50% bleach and then fixing them in 5% glutaraldehyde (Polysciences Inc, Warrington, PA) and heptane (Sigma). After manual devitellinization, embryos were fixed in 4% glutaraldehyde and 2% acrolein (Polysciences) in 0.1 M cacodylate buffer (Sigma). Devitellinized embryos were transferred to a chilled mixture of 1% osmium tetroxide (Polysciences) and 2% glutaraldehyde in 0.1 M cacodylate buffer, and then post-fixed in 1% osmium tetroxide in 0.1 M cacodylate buffer. Fixed embryos were dehydrated and embedded in Epon as previously described (Myat and Andrew, 2000). 65 nm thin sections, obtained on a Reichart-Jung Ultracut E, were stained with 2% uranyl acetate (Polysciences) and lead citrate (Polysciences) before viewing on a Phillips CM120 transmission electron microscope.

RESULTS

fkh is expressed early and continuously in the salivary gland secretory cells

fkh is proposed to play a major role in salivary gland determination and morphogenesis based on the failure of the salivary glands to internalize in *fkh* mutant embryos (Weigel et al., 1989a) and on FKH's repression of *trachealess* (*trh*), which encodes a duct-specific transcription factor (Isaac and Andrew, 1996), in the secretory cells (Kuo et al., 1996). To study FKH's function in detail, we began by analyzing its

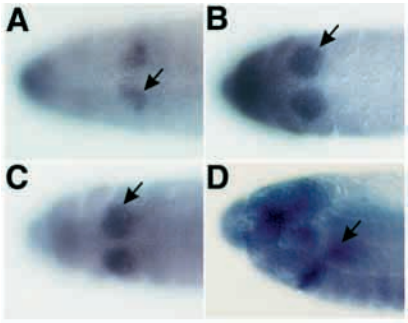

Fig. 1. *fkh* mRNA is expressed early and continuously in the salivary secretory cells. (A) *fkh* mRNA is first detected during embryonic stage 9 in a ventral-posterior region (arrow) of the secretory placode. (B) *fkh* mRNA is observed in all cells of the secretory primordia by embryonic stage 10 (arrow). (C,D) *fkh* mRNA is detected in secretory cells during early stage 11 when invagination begins (C, arrow) and in the internalized salivary tube (D, arrow) of stage 12 wild-type embryos. A, B and C are ventral views and D is a lateral view.

expression in the salivary gland throughout embryogenesis. *fkh* mRNA was first detected during embryonic stage 9 in the ventral-posterior cells of the secretory placode (Fig. 1A). *fkh* mRNA was detected at approximately equivalent levels in all secretory cells from early embryonic stage 10 (Fig. 1B) and throughout embryogenesis (Fig. 1C,D and data not shown). FKH is expressed in the salivary glands of late third instar larvae (Kuzin et al., 1994) where it activates expression of the *Salivary gland secretion protein 3* (*Sgs3*) and *Salivary gland secretion protein 4* (*Sgs4*) genes (Lehmann and Korge, 1996; Mach et al., 1996). This late expression suggests that *fkh* is expressed in the salivary gland throughout the larval stages until the onset of metamorphosis.

Secretory cells are not internalized in *fkh* mutants

To characterize the role of *fkh* in salivary gland morphogenesis, we analyzed both whole-mount embryos and histological sections of salivary glands from wild-type and *fkh* mutants stained with a secretory cell marker, dCREB-A (Andrew et al., 1997). In wild-type embryos, salivary glands are internalized through a series of coordinated cell shape changes that begin with cells in the dorsal-posterior region of the primordium (Myat and Andrew, 2000; Fig. 2A,B). A wave of cell shape changes extends to the dorsal-anterior, then the ventral-anterior, and, finally, the ventral-posterior cells of the placode, resulting in the internalization of the entire primordium (Fig. 2E,F). Once the ventral-posterior cells are internalized, the cells at the distal end of the secretory tube appear to turn and migrate posteriorly (Fig. 2F), ultimately positioning the salivary glands along the anterior-posterior body axis (Fig. 2I,J). In *fkh* mutants, relatively normal salivary primordia were observed. However, distinct invaginating pits, which are normally seen in wild-type salivary glands at this stage (Fig. 2A,B), were not visible in *fkh* mutants (Fig. 2C,D). At later stages, the size of the *fkh* secretory placode and the levels of dCREB-A staining were reduced (Fig. 2G,H). Even at late embryonic stages, dCREB-A-positive secretory cells were still located at or near the embryo surface of *fkh* mutants (Fig. 2K,L), confirming the failure to invaginate.

Comparisons of histological sections of wild-type and *fkh* embryos revealed three differences in the secretory primordia and surrounding tissues. (1) Wild-type salivary placode cells were uniformly columnar (Fig. 3A,B), whereas the *fkh* salivary placode cells were a mixture of round and columnar cells, with the ventral-most region consisting mostly of round cells (Fig. 3E-H). (2) wild-type secretory cells were always in a monolayer (Fig. 3A-D) while many of the *fkh* mutant cells were found in multiple layers with some cells apparently

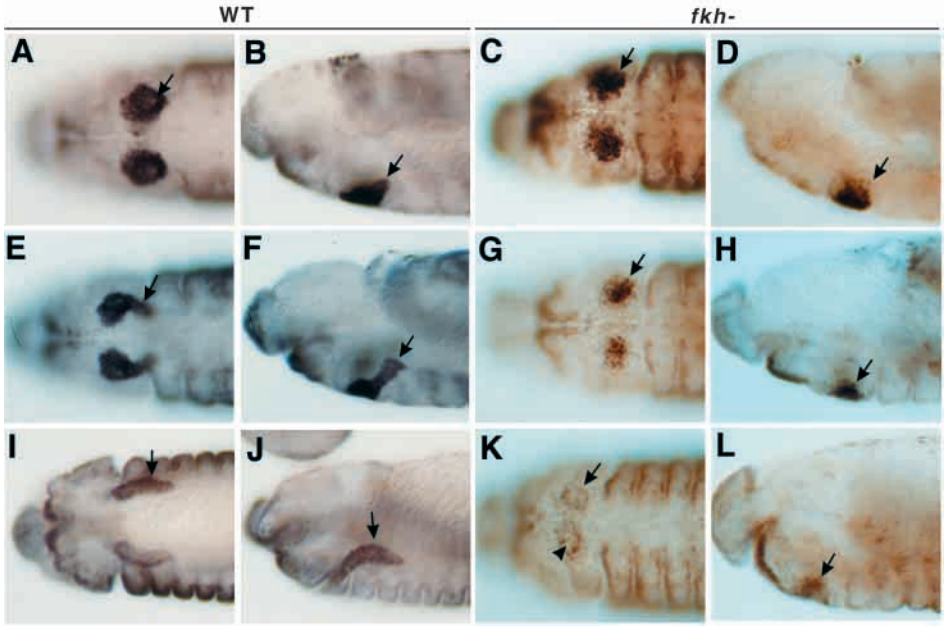

Fig. 2. Salivary secretory cells do not internalize in *fkh* mutant embryos. Wild-type (A, B, E, F, I and J) and *fkh* mutant (C, D, G, H, K and L) embryos were stained with antiserum to dCREB-A. A,C,E,G,I and K are ventral views; B,D,F,H,J and L are the corresponding lateral views of the same embryos. (A,B) Secretory cell invagination in wild-type embryos begins during early embryonic stage 11 in the dorsal-posterior region of the primordia (arrows). (C,D) Although a normal secretory placode forms in *fkh* mutant embryos, an invaginating pit is not evident during stage 11 (arrows). (E,F) During embryonic stage 12, the internalized wild-type secretory cells form a tube that is directed dorsally (arrows). (G,H) In stage 12 *fkh* mutant embryos, fewer dCREB-A-positive cells are observed and these cells are found at the embryo surface (arrows). (I,J) At stage 13, when internalization is complete, wild-type embryos have elongated salivary secretory tubes, which lie along the anterior-posterior axis (arrows). (K,L) At the same stage, two rings of weakly staining dCREB-A-positive cells (arrows) surrounding central pits (K, arrowhead) are observed near the ventral surface of *fkh* mutant embryos.

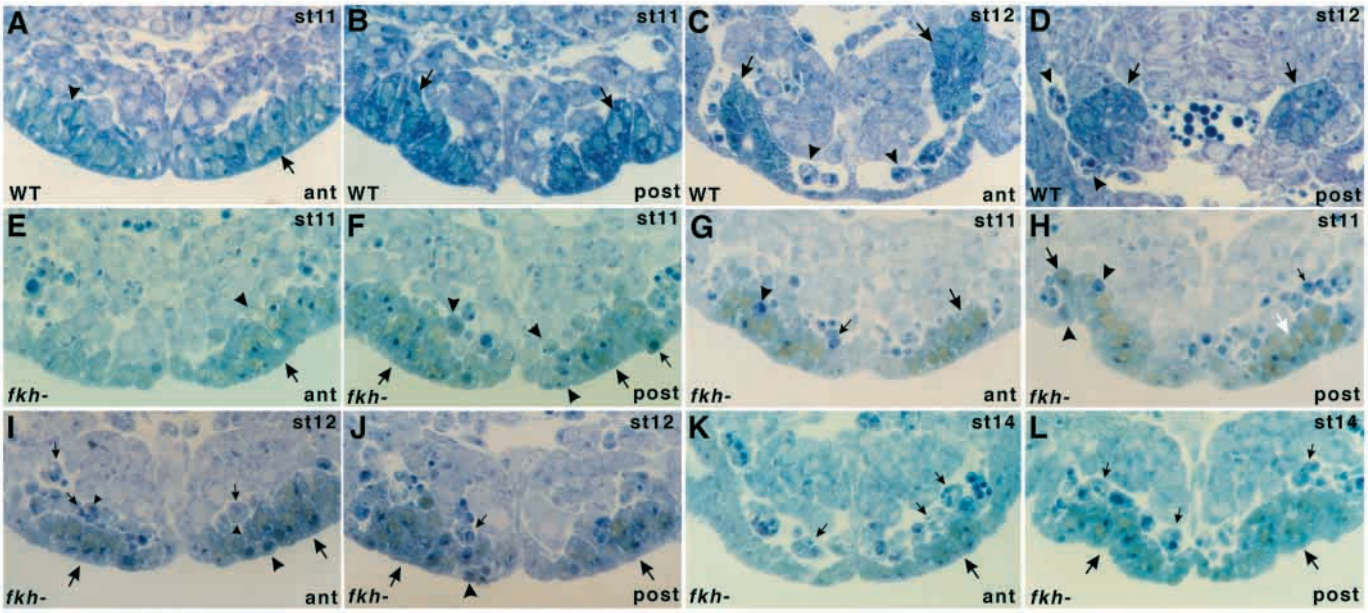

Fig. 3. *fkh* mutant embryos show morphological signs of extensive salivary gland cell death. 1 μm sections of salivary glands stained with α-dCREB-A and counter-stained with Toluidine-Blue are shown. A-D are wild-type embryos; E-L are *fkh* mutant embryos. A,C,E,G,I and K are representative cross sections from the anterior (ant) regions; B,D,F,H,J and L are representative cross sections from the posterior (post) regions of the same glands. (A) Cells from the anterior region of wild-type secretory placodes at stage 11 are elongated with nuclei in either the apical (arrow) or the basal (arrowhead) domains of the cells. (B) The dorsal-posterior cells of wild-type embryos are wedge-shaped with basal nuclei (arrows). (C,D) The internalized secretory cells of stage 12 wild-type embryos form an elongated tube with a single layer of cells surrounding a central lumen (arrows). Oval-shaped macrophage-like cells are detected in the periphery of the secretory tube (arrowheads). (E,F) Cells in early stage 11 secretory placodes of *fkh* embryos are either elongated (large arrows) or round (arrowheads and small arrow). (G,H) In *fkh* embryos at late stage 11, pyknotic structures that stain intensely with Toluidine Blue are found within the secretory epithelium (arrowheads) and in the space between the secretory cells and the surrounding tissue (small arrows). The dorsal-anterior cells are elongated (G, large arrow), while the dorsal-posterior cells are sometimes wedge-shaped (H, large black arrow) and sometimes columnar (H, white arrow). (I,J) During stage 12, the dorsal cells are elongated (large arrows), whereas the ventral cells are round and stacked on each other (arrowheads). Macrophage-like cells (small arrows) that sometimes show dCREB-A staining (I, small arrowheads) are found adjacent to the secretory cells. (K,L) During stage 14, secretory cells of *fkh* mutants (large arrows) are found at the ventral surface surrounded by oval-shaped macrophage-like cells (small arrows). Some of the secretory cells appear to be wedge-shaped and a shallow indentation at the ventral surface is observed (L, large arrows). A minimum of three wild-type and *fkh* embryos was sectioned for each embryonic stage shown.

dissociating from the salivary epithelium (Fig. 3E-L). (3) Very few macrophage-like cells or pyknotic structures were observed near the wild-type secretory primordia (Fig. 3C,D), whereas numerous macrophage-like cells and pyknotic structures were observed surrounding the salivary primordia in the *fkh* mutants (Fig. 3G-L). Many of the macrophage-like cells in the *fkh* mutants (Fig. 3I,J, small arrows) showed variable levels of dCREB-A staining (Fig. 3I, arrowheads), suggesting that these cells may have engulfed dCREB-A positive secretory cells. Interestingly, *fkh* secretory cells in the dorsal-posterior region of the placode (Fig. 3F,H,J,L) had nuclei in a basal position, as in wild-type embryos (Fig. 3B,D). However, despite this nuclear translocation, most *fkh* cells remained columnar (Fig. 3H,J,L) rather than becoming wedge-shaped, as occurs in wild-type salivary glands.

The salivary gland cells of *fkh* mutants die through an apoptotic mechanism

To determine whether the oval-shaped cells observed in or near the secretory placodes of *fkh* mutants were macrophages, we stained for the macrophage marker protein, CROQUEMORT (CRQ; Franc et al., 1999). During embryonic stage 11, a few CRQ-positive cells were found in the region of the secretory primordia of wild-type embryos (Fig. 4A). In contrast, many more CRQ-positive cells were found in or near the secretory primordia of *fkh* mutants (Fig. 4C). At the end of invagination, we observed CRQ-positive cells near the internalized secretory cells of wild-type embryos (Fig. 4B), suggesting that low levels of apoptosis may occur normally in the region of the salivary glands. However, significantly more CRQ-positive cells were observed in the region of the secretory primordia in *fkh* mutants (Fig. 4D). The CRQ-positive cells observed in whole-mount embryos are likely to correspond to the oval-shaped cells observed in histological sections. This finding suggested an increased recruitment of circulating macrophages to the salivary glands of *fkh* mutants compared to wild type. Since macrophages are professional phagocytes that engulf dying cells (Tepass et al., 1994; Morrissette et al., 1999), their presence suggested a significant increase in cell death in the salivary glands of *fkh* mutants compared to wild type.

To verify the increased cell death of secretory cells in *fkh* mutants and to determine whether the cells were dying by apoptosis or necrosis, we examined the expression of three *Drosophila* death genes, *reaper* (*rpr*), *grim* and *head involution defective* (*hid*), in both wild-type and *fkh* mutant embryos. *rpr*, *grim* and *hid* encode proteins that function near the top of the

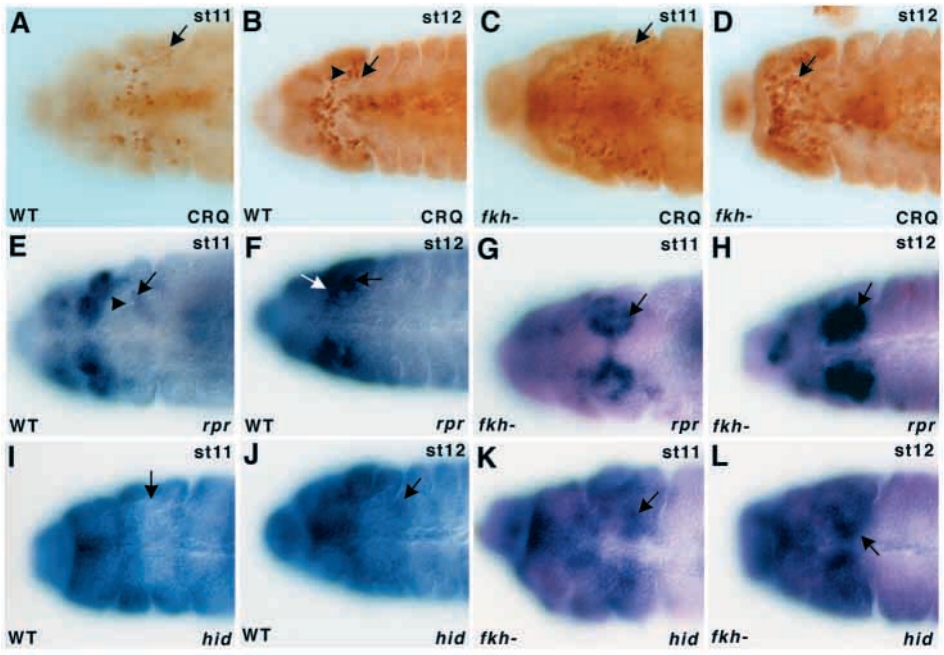

Fig. 4. Macrophages and *rpr* and *hid* mRNA levels accumulate in the secretory primordia of *fkh* mutant embryos. Wild-type (A,B) and *fkh* mutant (C,D) embryos were stained with antiserum to Crq. At stage 11, relatively few Crq-positive cells are observed in the region of the wild-type secretory placode (A, arrow) compared to *fkh* embryos (C, arrow). (B) In stage 12 wild-type embryos, Crq-positive cells (arrowhead) are found adjacent to the internalized secretory tube (arrow). (D) Many Crq-positive cells are found within and around the secretory epithelium in *fkh* embryos at a similar stage (arrow). (E) In stage 11 wild-type embryos, *rpr* mRNA is detected at low levels (arrow) in cells immediately posterior to the invaginating pit (arrowhead). (F) As the salivary gland is internalized during stage 12, *rpr* mRNA levels in the posterior cells increase (arrow) and *rpr* mRNA is observed in a few cells anterior to the invaginating pit (white arrow). *rpr* mRNA is not detected in the internalized secretory cells, which are not in the plane of focus. (G,H) Stage 11 and 12 *fkh* mutant embryos show significantly increased levels of *rpr* mRNA in the salivary placode (arrows). During stage 11, the level of *hid* mRNA in the wild-type secretory placode (I, arrow) is lower than in surrounding non-salivary gland cells. As the cells internalize during stage 12, *hid* mRNA levels increase slightly, particularly in cells posterior to the invaginating pit (J, arrow). *fkh* embryos show increased levels of *hid* mRNA in the salivary placode during stage 11 (K, arrow) and 12 (L, arrow). All panels show ventral views of embryos.

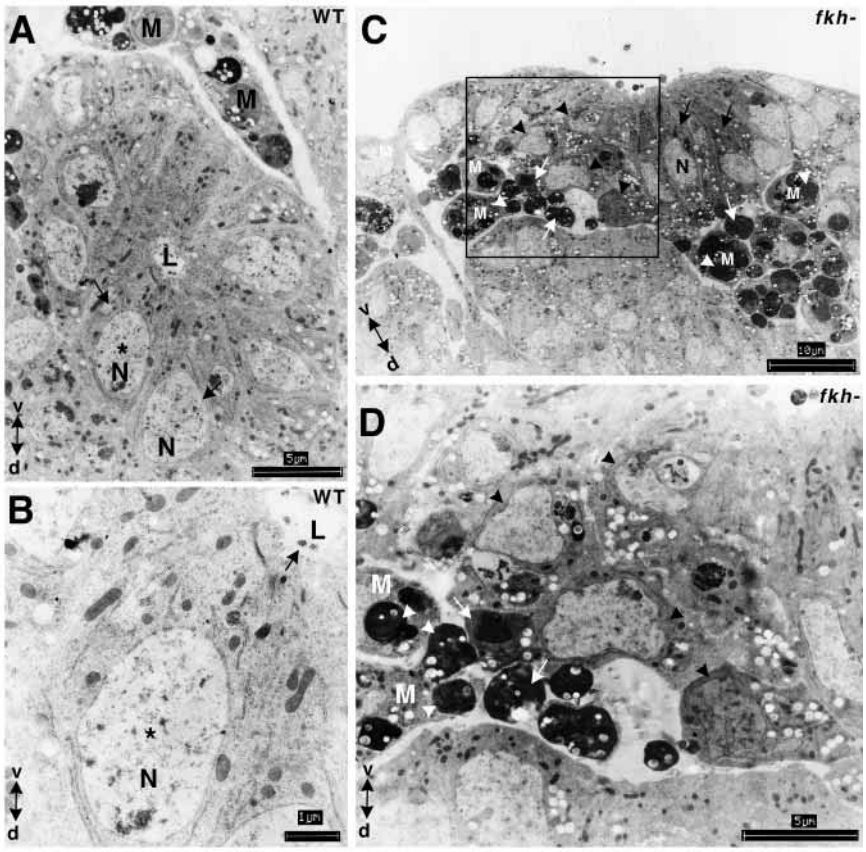

Fig. 5. Apoptotic bodies and macrophages are found in the secretory placode of *fkh* mutants. (A) A representative cross section of a wild-type salivary gland at stage 13 shows columnar cells (arrows) surrounding a central lumen (L). (B) A magnified view of a wild-type secretory cell from A (asterisk) shows the nucleus (N) is located basally and the constricted apical surface faces the lumen (L) which contains secretory products (arrow). (C) In *fkh* embryos at stage 13, the dorsal secretory cells are elongated (black arrows) while the ventral secretory cells are round (black arrowheads). Apoptotic bodies with condensed nuclei and cytoplasm (white arrows) are found within the secretory epithelium of *fkh* mutants. Numerous macrophages (M) that have engulfed apoptotic bodies (white arrowheads) surround the dying secretory cells. A magnified view (D) of the boxed ventral region in C shows *fkh* secretory cells that have lost their columnar morphology (black arrowheads), apoptotic cells (white arrows), and macrophages (M) engulfing apoptotic bodies (white arrowheads). 65 nm sections were obtained from a minimum of three wild-type and *fkh* embryos at stage 13. v, ventral; d, dorsal.

Drosophila cell death pathway and induce a cascade of caspase activation (reviewed by Abrams, 1999; Song and Steller, 1999). Expression of *rpr*, *grim* and *hid* precedes apoptotic cell death and the absence of these genes eliminates the cell death that normally occurs during embryogenesis (White et al., 1994; Grether et al., 1995; Chen et al., 1996). In wild-type embryos, *rpr* RNA was initially detected in only a small group of secretory cells found posterior to the invaginating pit (Fig. 4E). At the end of invagination in wild-type embryos, *rpr* RNA was detected at relatively high levels in the few secretory cells remaining at the ventral surface, but not in the internalized secretory cells (Fig. 4F). In early *fkh* mutants, *rpr* RNA levels were significantly increased in all cells except those in a dorsal-anterior position in the primordia (Fig. 4G). Slightly later, high levels of *rpr* RNA were detected in all secretory cells of *fkh* mutants (Fig. 4H). *hid* RNA levels were also increased in *fkh* relative to wild type. Early *fkh* embryos showed increased *hid* expression levels in an apparently random array of secretory cells (Fig. 4K) compared to wild-type embryos at the same stage, in which *hid* expression levels were lower in the secretory cells than they were in the surrounding non-salivary gland tissues (Fig. 4I). At later stages, slightly increased levels of *hid* RNA were detected in wild-type embryos, particularly in the posterior cells that also had relatively high levels of *rpr* expression (Fig. 4J). High levels of *hid* RNA were detected at later stages in all *fkh* mutant secretory cells, with particularly high levels in the ventral primordia (Fig. 4L). Unlike *rpr* and *hid*, *grim* RNA was not detected in the secretory primordia of either wild-type or *fkh* embryos (data not shown).

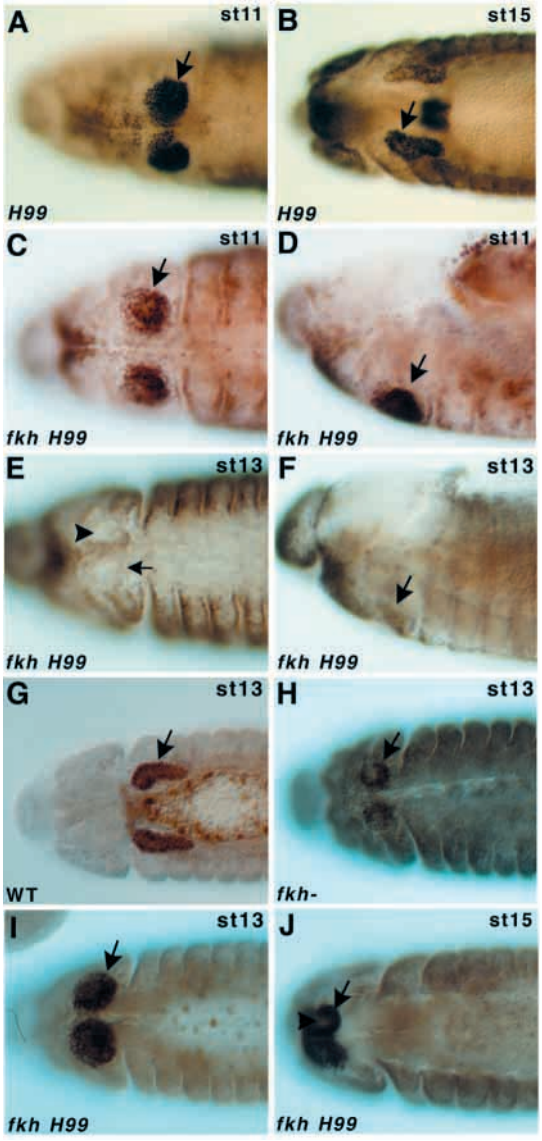

Fig. 6. Secretory cells survive in *fkh H99* mutant embryos. (A,B) *H99* embryos were stained for dCREB-A. *fkh H99* mutant embryos were stained either for dCREB-A (C-F) or PS (I,J). Wild-type (G) and *fkh* (H) mutant embryos were stained for PS. A normal secretory placode (A, arrow) and secretory tubes (B, arrow) are formed in *H99* embryos. (C,D) All cells in the early secretory placode of *fkh H99* embryos express dCREB-A (arrows). (E,F) Secretory cells of late *fkh H99* embryos form a pit (arrowhead) but no longer express dCREB-A. (G) PS is expressed in the secretory tubes of wild-type embryos (arrow). (H) PS is expressed in two rings of cells surrounding central pits in late *fkh* embryos (arrow). (I,J) PS is expressed in all secretory cells of early *fkh H99* embryos (I, arrow), and in the secretory cells (J, arrow) surrounding central pits (J, arrowhead) in late *fkh H99* embryos. A-C,E, and G-J are ventral views; D and F are the corresponding lateral views of C and E, respectively.

The increased levels of both *rpr* and *hid* in the secretory primordia suggested that in the absence of *fkh* function, secretory cells die by apoptosis. In support of an apoptotic mechanism of cell death, TEM analyses revealed that *fkh* mutant salivary glands showed cytological changes characteristic of apoptosis (Abrams et al., 1993). For example, *fkh* secretory cells, particularly those in the ventral part of the placode, had separated from neighboring cells and demonstrated nuclear condensation, cytoplasmic shrinkage and fragmentation (Fig. 5C,D, white arrows and black arrowheads). In addition, numerous macrophages with ingested apoptotic bodies were observed near the secretory cells of *fkh* mutants (Fig. 5C,D, white arrowheads). This is in contrast to the secretory cells of wild-type embryos, which at an equivalent stage, were found as a monolayer of wedge-shaped cells surrounding a central lumen (Fig. 5A,B). We observed very few macrophages or apoptotic bodies adjacent to the wild-type salivary glands.

fkh plays a dual role in salivary morphogenesis

The apoptotic cell death observed in the early secretory primordia of *fkh* mutants indicated that *fkh* was required for secretory cell survival (Figs 3-5). Thus, secretory cells may fail to invaginate in *fkh* mutants simply because the cells are dead or dying. Indeed, the ectopic expression of *rpr* and *hid*, but not grim, is effective in inducing early secretory cell death, which if extensive enough, prevents internalization (data not shown). Alternatively, *fkh* may have two separate roles in the salivary gland, one to promote cell survival and another to control invagination of the primordia. To distinguish between these possibilities, we rescued the apoptotic secretory cell death in *fkh* mutants by generating embryos that were mutant for *fkh* and also carried *Df(3L)H99*, a small deficiency that deletes *rpr*, *hid* and *grim* (*fkh H99*; White et al., 1994). Normal salivary glands were formed in embryos homozygous for *Df(3L)H99* (*H99*; Fig. 6A,B). In the *fkh H99* embryos, dCREB-A staining was detected in the entire secretory placode at early stages (Fig.

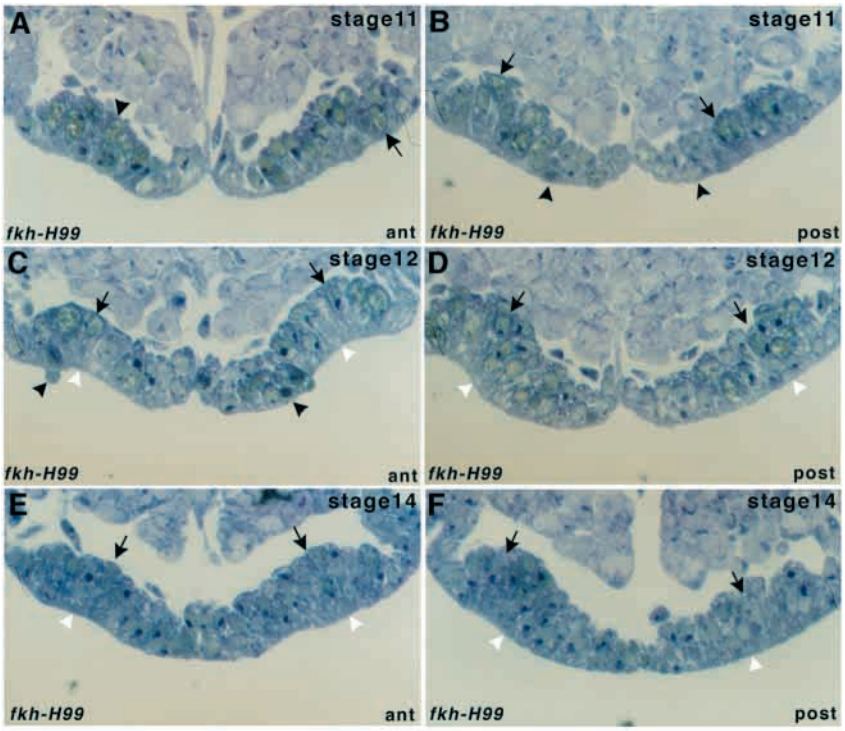

Fig. 7. Secretory cells of *fkh H99* embryos are not internalized. 1 μm sections from either the anterior (ant; A,C,E) or posterior (post) parts (B,D,F) of the same *fkh H99* secretory placode are shown. (A) Cells in the anterior regions of the placode have nuclei in both apical (arrows) and basal (arrowheads) regions of the cell. (B) Nuclei in the dorsal-posterior region of the primordia are positioned basally (arrows). Although many cells are columnar, round cells stacked on one another are observed, particularly in the ventral regions of the placode (arrowheads). (C,D) By embryonic stage 12, nuclei in both the dorsal-anterior and dorsal-posterior regions of the placode are basally positioned (large arrows). However, none of the elongated cells show evidence of apical constriction (white arrowheads). Some small, round cells are observed near the surface (C, black arrowheads). (E,F) By embryonic stage 14, most of the elongated cells have basal nuclei (large arrows) and the cells still show no evidence of apical constriction (white arrowheads). A minimum of three wild-type and *fkh* embryos was sectioned for each embryonic stage shown.

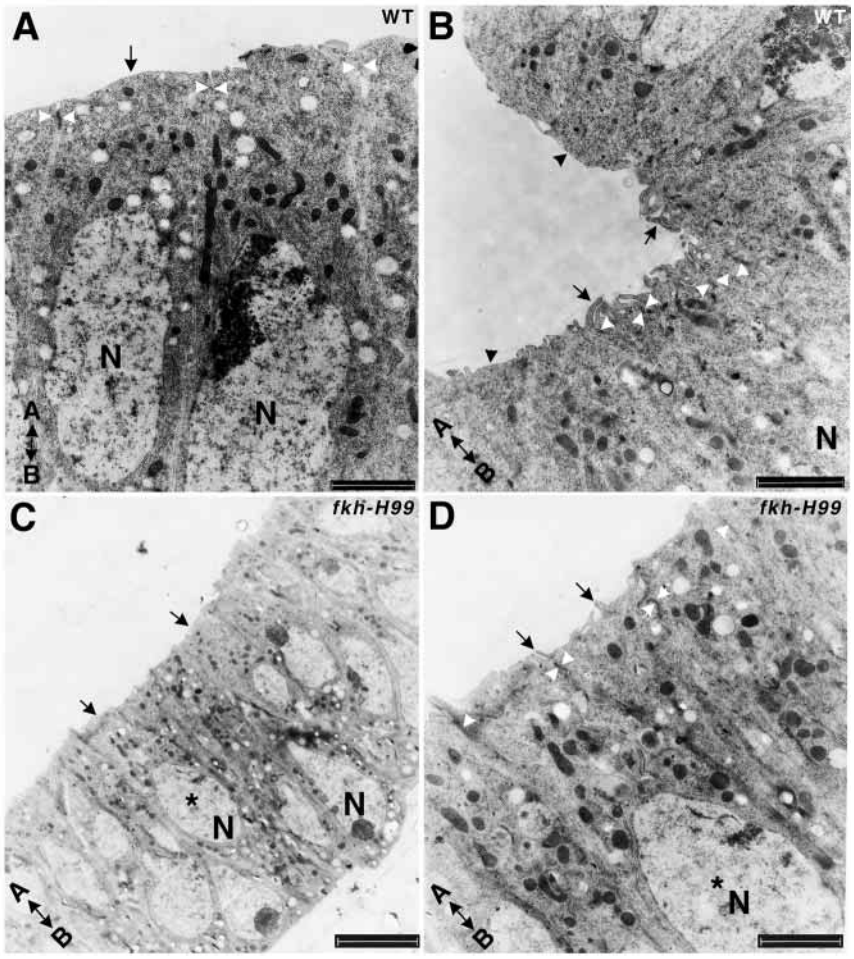

Fig. 8. Transmission electron micrographs of wild-type and *fkh H99* secretory cells. (A) The unconstricted apices (white arrowheads) of secretory cells from early stage 11 wild-type embryos are flat and broad (arrow). (B) The invaginating dorsal-posterior cells of wild-type embryos at late stage 11 have constricted their apices (white arrowheads) and extend numerous membrane protrusions at their apical surfaces (large arrows). Cells surrounding the invaginating pit have broad and flat apices (black arrowheads). (C) Secretory cells of *fkh H99* embryos at stage 12 have flat and broad unconstricted apices (large arrows) although nuclei (N) are located basally. (D) Magnified view of a representative cell from C (asterisk) shows unconstricted apices (white arrowheads) with a few membrane protrusions (black arrows). Constricted apical surfaces of invaginating wild-type secretory cells at stage 11 measure approximately 1.5 μm with an area of 1.76 μm^2 (n=21 cells from 3 different embryos), while unconstricted apical surfaces of *fkh H99* secretory cells at stage 12 measure approximately 2.6 μm with an area of 5.3 μm^2 (n=49 cells from 3 different embryos). White arrowheads indicate cell borders. N, nucleus; A, apical; B, basal. Scale bars in A, B and D represent 2 μm, while the scale bar in C represents 5 μm.

6C,D). This staining completely disappeared by embryonic stage 13 (Fig. 6E,F), suggesting that either *fkh* is required to maintain dCREB-A expression or that the *fkh H99* secretory cells are still dying. To address this issue, we analyzed the expression of another secretory marker protein, PS, whose expression was thought to be *fkh* independent (Seshaiah et al., unpublished data). In wild-type embryos, PS was expressed at high levels in the salivary glands throughout embryogenesis (Fig. 6G; P. Seshaiah, B. Miller and D. J. A., unpublished data). In *fkh* mutant embryos, PS was initially expressed in the entire secretory placode (data not shown), and at reduced levels in the surviving ring of secretory cells (Fig. 6H). Importantly, PS was expressed to very high levels in all secretory cells throughout embryogenesis in the *fkh H99* embryos (Fig. 6I,J). Nonetheless, the PS-expressing cells in the *fkh H99* embryos were not internalized and remained at their site of origin on the ventral surface (Fig. 6J). Therefore, in addition to its early role in promoting secretory cell survival, FKH is also required for the invagination of the secretory cells.

Histological sections and TEM analyses of *fkh H99* embryos confirmed the failure of the secretory cells to be internalized and revealed additional changes in the salivary glands (Figs 7 and 8). Cells of the *fkh H99* placode were columnar like the wild-type cells (compare Fig. 7A,B with Fig. 3A,B), except for cells in the ventral-posterior portion of the placode, which were round and stacked on one another (Fig. 7B). Interestingly, although coordinate nuclear migration occurred in the secretory cells of all *fkh H99* embryos in approximately the same temporal and spatial pattern as in wild type, the apical surface membranes failed to constrict even at very late stages (Fig. 7C-F). Consequently, the invaginating pits of *fkh H99* salivary glands were wide and shallow compared to those of wild-type embryos. We confirmed the absence of apical membrane constriction by analyzing transmission electron micrographs of invaginating wild-type and *fkh* secretory cells. Prior to invagination, wild-type secretory cells have broad and flat apices (Fig. 8A, arrow). Wild-type secretory cells at the center of the invaginating pit have constricted apices, and showed numerous membrane protrusions at the apical surface (Fig. 8B, white arrowheads and black arrows). In contrast, secretory cells at the lateral edges of the invaginating pit, have flat and broad apices with few membrane protrusions (Fig. 8B, black arrowheads). In late *fkh H99* embryos, the apices of the secretory cells were unconstricted and appeared flat and broad (Fig. 8C, arrows), similar to the apices of secretory cells in early wild-type embryos (Fig. 8A, arrow). Fewer apical membrane protrusions are found at the surface of *fkh H99* secretory cells compared to wild type (Fig. 8D, arrows). Altogether, these findings suggested that *fkh* is required for secretory cells both to survive and to invaginate. Moreover, the absence of apical membrane constriction may be the underlying defect in the failure of *fkh* mutant salivary glands to internalize.

DISCUSSION

fkh secretory cells die by apoptosis

We have shown that salivary glands do not form in *fkh* mutants in part because the secretory cells die by apoptosis. Apoptosis of the *fkh* secretory cells was detected as early as stage 11 and was still apparent at stage 14. Cells in the ventral-most region of the *fkh* mutant placodes were the first to express *rpr* (Fig. 4G) and showed the earliest morphological abnormalities; cells were frequently round, instead of columnar, and were no longer in an epithelial monolayer (Fig. 3E-J). Cells in the more dorsal regions of the placode were elongated, were in a monolayer and underwent basal nuclear migration at approximately the appropriate developmental stage (Fig. 3E-J). However, at later stages, the dorsal cells of the *fkh* mutant salivary glands showed the same morphological abnormalities as observed in ventral cells at earlier stages (Fig. 3K,L), consistent with the relatively delayed expression of *rpr* in these cells (Fig. 4H). The time difference may reflect when FKH function is required for survival in the ventral versus dorsal primordia. Indeed, *fkh* expression is initiated in the ventral-most cells and only later expands to the rest of the secretory primordia (Fig. 1).

The early expression of *rpr* and *hid* in the secretory primordia and the pattern of cell death in *fkh* mutants indicate that cell death is not induced because of a failure of *fkh* secretory cells to change shape and invaginate. Expression of both *rpr* and *hid*, and morphological signs of apoptosis were detected in the *fkh* secretory placode well before these cells would normally change shape. Moreover, apoptosis in *fkh* embryos occurred first in the ventral secretory cells which are normally the last cells to change shape and invaginate in wild-type embryos. In the absence of *fkh*, expression of *rpr* and *hid* are elevated, suggesting that FKH prevents apoptosis by suppressing *rpr* and *hid* expression, either directly or indirectly, and that expression of both *rpr* and *hid* is responsible for the extensive secretory cell death observed in *fkh* mutants. The normal expression of *rpr* and *hid* in the posterior-most secretory cells in wild-type embryos suggests that some regulated cell death may normally occur, even though *fkh* levels remain high in all secretory cells. The posterior-most secretory cells that first express *rpr* (Fig. 4E) and that later express both *rpr* and *hid* (Fig. 4F,J) may remain at the embryo surface during the internalization of the remainder of the secretory primordia to provide an anchor to the surrounding ectoderm. At the end of invagination when all cells of the placode have been internalized, we postulate that these posterior-most cells may undergo apoptosis, which would separate the internalized secretory cells from the epidermis. This separation would then allow the posterior secretory cells to form contacts with the duct cells, which internalize after the secretory cells and form the tubes that connect the secretory cells to the larval mouth (for review, see Andrew et al., 2000).

fkh may promote cell survival not only in the salivary gland, but also in the anterior and posterior midgut. In *fkh* mutants most of the midgut epithelium degenerates and is infiltrated by a large population of macrophage cells (Weigel et al., 1989; Tepass et al., 1994). Interestingly, the *C. elegans* HNF-3/FKH homolog, *daf-16*, acts downstream of the insulin-receptor signaling pathway to double life span (Lin et al., 1997; Hsin and Kenyon, 1999). Perhaps certain members of the FKH family of transcription factors function to promote survival both at the cellular and whole organismal levels.

fkh is required for apical membrane constriction

The formation of an ectodermally derived organ, such as the *Drosophila* salivary gland, requires that the primordia initially found at the surface of the embryo invaginate to form an

internalized structure. Our previous work demonstrated that salivary secretory cell invagination occurs in a regulated and sequential manner, most likely by an apical constriction mechanism (Myat and Andrew, 2000). In contrast to HKB, a transcription factor that regulates the order of cell shape changes in the secretory placode (Myat and Andrew, 2000), FKH appears to mediate the actual cell shape changes. In *fkh H99* embryos, where secretory cells are kept alive by the removal of death genes, secretory cells fail to constrict their apical surface membranes and, therefore, do not change shape and internalize (Figs 7, 8). In contrast, cells in the dorsal-posterior region of the *fkh* placode did occasionally constrict their apical surface membranes, thus forming a distinct invaginating pit like those of wild-type salivary glands (Fig. 3H,L). The failure of secretory cells in *fkh H99* embryos to constrict their apical surface membranes, while their counterparts in *fkh* embryos are occasionally able to do so, could be explained by the extensive cell death in the secretory placode of *fkh* mutants. By the time *fkh* secretory cells start to constrict, a significant number of secretory cells have already died and been cleared away by macrophages. The presence of fewer secretory cells in the placode could reduce the surface tension in the epithelium, thus facilitating apical constriction of the remaining secretory cells. In contrast, when the normal number of secretory cells is restored in *fkh H99* embryos by blocking apoptosis, the same physical constraints exist in the secretory epithelium as in wild-type embryos, and due to the absence of *fkh* function, cells fail to constrict their apical membrane. Alternatively, the cells that appear wedge-shaped in the *fkh* mutants may actually be dying cells that are not able to maintain their shape. These dying cells may collapse and remain broad only in basal regions, where the nuclei are found.

While apical membranes failed to constrict in the secretory cells of *fkh H99* embryos, nuclear migration was not affected (Figs 7 and 8). It was previously not possible to discern whether the basal migration of nuclei and the constriction of the apical membrane were two separate events that contributed independently to cell shape change, or whether one event depended on the other. Live imaging of cell shape changes during *Drosophila* gastrulation using three-dimensional fluorescence microscopy showed that in some cases, nuclei moved basally in the absence of apical constriction, suggesting that these two processes can be independent (Kam et al., 1991). Our histological and TEM data of *fkh H99* embryos confirm that nuclear migration and apical membrane constriction are indeed two separate events and that apical constriction does not occur simply because of basal nuclear movement (Figs 7 and 8). Ultrastructural and immunocytochemical data from a variety of epithelia that undergo apical constriction indicate that the apical contractile machinery consists of an actin-myosin network (Bement et al., 1993; Young et al., 1991, 1993). This model is supported by experiments where cytochalasin, an actin-depolymerizing agent, arrests or reverses invagination (Wrenn, 1971; Karfunkel, 1972; Spooner and Wessells, 1972; Morriss-Kay, 1981). Similar effects are observed with calcium treatment of invaginating epithelia (Ash et al., 1973; Moran, 1976; Moran and Rice, 1976; Brady and Hilfer, 1982). Since the basal movement of nuclei is linked to the microtubule network (Messier, 1978), and the constriction of the apical membrane is linked to the actin filament system, it is possible that FKH functions in a signal transduction pathway that specifically targets actin. TEM data of wild-type embryos at different stages of salivary secretory cell invagination demonstrated that constriction of the apical surface membrane was accompanied by dynamic membrane protrusions at the apical surface (Fig. 8B and data not shown). These data support the apical constriction model for invagination which predicts that apical membrane protrusions form as a result of the actomyosin-driven contraction of the apical domain. However, it is still possible that active secretion and cell-cell adhesion also contribute significantly to the inward folding of the epithelium. Thus, the *fkh H99* embryos, in which apical membrane constriction is specifically abrogated, provide a valuable tool with which we can further address the roles of apical constriction, apical secretion and cell-cell adhesion in epithelial invagination.

FKH function during *Drosophila* development

Our studies on *Drosophila* FKH demonstrate two roles during development of the embryonic salivary glands, one in cell survival and another in apical membrane constriction. Among the known targets of FKH in the salivary gland are two genes that also encode transcription factors, *trh* (Isaac and Andrew, 1996; Kuo et al., 1996) and *dCREB-A* (this work), and two salivary gland glue protein genes, *Sgs3* and *Sgs4* (Lehmann and Korge, 1996; Mach et al., 1996). *trh* is expressed and required in the duct cells and its initial expression in the secretory cells is later repressed by FKH (Isaac and Andrew, 1996; Kuo et al., 1996). Early expression of dCREB-A is FKH-independent; however, later expression of dCREB-A requires FKH, especially in cells rescued from programmed cell death (Fig. 6). None of these downstream target genes is likely to mediate FKH's roles in cell survival and/or apical membrane constriction. *Sgs3* and *Sgs4* are not expressed until several days after salivary gland internalization (Lehmann, 1996). Secretory cell survival and internalization are completely normal in embryos lacking function of *trh* or *dCREB-A* (Isaac and Andrew, 1996; Andrew et al., 1997) and in embryos where *trh* is continuously expressed in the secretory cells (D. D. Isaac and D. J. A., unpublished observation). Thus, it is important to identify the target genes that mediate FKH's role in early secretory cell survival and morphogenesis. To this end, we are characterizing two recently identified genes whose expression in the salivary gland is FKH-dependent (E. Abrams and D. J. A., unpublished observation).

We wish to extend our thanks to P. Bradley, C. Machamer, and K. Wilson for their constructive criticisms of the manuscript. We thank J. Abrams, E. Baehracke, J. Nambu and H. Steller for fly stocks and cDNA constructs. We thank K. White for the α-CRQ antisera. We thank C. Cooke for training M. M. M. in TEM. We thank the C. Goodman Laboratory for TEM fixation protocols. We thank the other members of the Andrew lab for their material and intellectual contributions to the work. This work was supported by an NIH grant to D. J. A. (RO1 GM51311) and a Jane Coffin Childs postdoctoral fellowship to M. M. M.

REFERENCES

Abrams, M. J., White, K., Liselotte, I. F. and Steller, H. (1993). Programmed cell death during *Drosophila* embryogenesis. *Development* **117**, 29-43.

Abrams, J. M. (1999). An emerging blueprint for apoptosis in Drosophila. *Trends Cell Biol.* **9**, 435-440.

Andrew, D. J., Baig, A., Bhanot, P., Smolik, S. M. and Henderson, K. D. (1997). The *Drosophila dCREB-A* gene is required for dorsal/ventral patterning of the larval cuticle. *Development* **124,** 181-193.

Andrew, D. J., Henderson, K. D. and Seshaiah, P. (2000). Salivary gland development in Drosophila melanogaster. *Mech. Dev.* **92,** 5-17.

Ash, J. F., Spooner, B. S. and Wessells, N. K. (1973). Effects of papaverine and calcium-free medium on salivary gland morphogenesis. *Dev. Biol.* **33**, 463-469.

Barrett, K., Leptin, M. and Settleman, J. (1997). The Rho GTPase and a putative RhoGEF mediate a signaling pathway for the cell shape changes in Drosophila gastrulation. *Cell* **91,** 905-915.

Bement, W. M., Forscher, P. and Mooseker, M. S. (1993). A novel cytoskeletal structure involved in purse string wound closure and cell polarity maintenance. *J. Cell Biol* **121,** 565-578.

Brady, R. C. and Hilfer, S. R. (1982). Optic cup formation: a calcium-regulated process. *Proc. Natl. Acad. Sci. USA* **79,** 5587-5591.

Chen, P., Nordstrom, W., Gish, B. and Abrams, J. M. (1996). *grim*, a novel cell death gene in Drosophila. *Genes Dev.* **10,** 1773-1782.

Costa, M., Wilson, E. T., and Wieschaus, E. (1994). A putative cell signal encoded by the folded gastrulation gene coordinates cell shape changes during Drosophila gastrulation. *Cell* **76,** 1075-1089.

Ettensohn, C. A. (1985). Mechanisms of epithelial invagination. *Q. Rev. Biol.* **60,** 289-307.

Flybase (1999). The Flybase database of the Drosophila Genome Projects and community literature. The Flybase Consortium. *Nucleic Acids Res.* **27**, 85-88.

Franc, N. C., Heitzler, P., Ezekowitz, R. A. and White, K. (1999). Requirement for *croquemort* in phagocytosis of apoptotic cells in Drosophila. *Science* **284,** 1991-1994.

Fristrom, J. (1988). The cellular basis of epithelial morphogenesis. *Tissue Cell* **20,** 645-690.

Grether, M. E., Abrams, J. M., Agapite, J., White, K. and Steller, H. (1995). The *head involution defective* gene of Drosophila melanogaster functions in programmed cell death. *Genes Dev.* **9,** 1694-1708.

Gustafson, T. and Wolpert, L. (1962). Cellular mechanisms in the morphogenesis of the sea urchin larva. *Exp. Cell Res.* **27,** 260-279.

Hacker, U. and Perrimon, N. (1998). *DRhoGEF2* encodes a member of the Dbl family of oncogenes and controls cell shape changes during gastrulation in Drosophila. *Genes Dev.* **12,** 274-284.

Herman, T., Hartwieg, E. and Horvitz, H. R. (1999). *sqv* mutants of *Caenorhabditis elegans* are defective in vulval epithelial invagination. *Proc. Natl. Acad. Sci. USA* **96,** 968-973.

Herman, T. and Horvitz, H. R. (1999). Three proteins involved in *Caenorhabditis elegans* vulval invagination are similar to components of a glycosylation pathway. *Proc. Natl. Acad. Sci. USA* **96,** 974-979.

Hsin, H. and Kenyon, C. (1999). Signals from the reproductive system regulate the lifespan of *C. elegans*. *Nature* **399**, 362-366.

Isaac, D. D. and Andrew, D. J. (1996). Tubulogenesis in *Drosophila*: a requirement for the *trachealess* gene product. *Genes Dev.* **10,** 103-117.

Kam, Z., Minden, J. S., Agard, D. A., Sedat, J. W. and Leptin, M. (1991). Drosophila gastrulation: analysis of cell shape changes in living embryos by three-dimensional fluorescence microscopy. *Development* **112,** 365-370.

Karfunkel, P. (1972). The activity of microtubules and microfilaments in neurulation in the chick. *J. Exp. Zool.* **181,** 289-301.

Kuo, Y. M., Jones, N., Zhou, B., Panzer, S., Larson, V. and Beckendorf, S. K. (1996). Salivary duct determination in *Drosophila*: roles of the EGF receptor signaling pathway and transcription factors Fork head and Trachealess. *Development* **122,** 1909-1917.

Kuzin, B., Tillib, S., Sedkov, Y., Mizrokhi, L. and Mazo, A. (1994). The Drosophila *trithorax* gene encodes a chromosomal protein and directly regulates the region-specific homeotic gene *fork head*. *Genes Dev.* **8,** 2478-2490.

Lane, M. C., Koehl, M. A., Wilt, F. and Keller, R. (1993). A role for regulated secretion of apical extracellular matrix during epithelial invagination in the sea urchin. *Development* **117,** 1049-1060.

Lehmann, M. and Korge, G. (1996). The *fork head* product directly specifies the tissue-specific hormone responsiveness of the Drosophila *Sgs-4* gene. *EMBO J.* **15,** 4825-4834.

Lehmann, R. and Tautz, D. (1994). *In situ* Hybridization to RNA. In Drosophila melanogaster: *Practical Uses in Cell and Molecular Biology* (ed. L. B. S. Goldstein and E. A. Fyrberg), pp. 575-598. San Diego: Academic Press.

Leptin, M. (1999). Gastrulation in Drosophila: the logic and cellular mechanisms. *EMBO J.* **18,** 3187-3192.

Lin, K., Dorman, J. B., Rodan, A. and Kenyon, C. (1997). daf-16: an HNF-3/fork head family member that can function to double the lifespan of *Caenorhabditis elegans. Science* **278,** 1319-1322.

Mach, V., Ohno, K., Kokubo, H. and Suzuki, Y. (1996). The Drosophila Fork head factor directly controls larval salivary gland-specific expression of the glue protein gene *Sgs-3*. *Nucleic Acids Res.* **24,** 2387-2394.

Messier, P. E. (1978). Microtubules, interkinetic nuclear migration and neurulation. *Experientia* **34,** 289-296.

Mittenthal, J. E. and Mazo, R. M. (1983). A model for shape generation by strain and cell-cell adhesion in the epithelium of an arthropod leg segment. *J. Theor. Biol.* **100,** 443-483.

Moran, D. and Rice, R. W. (1976). Action of papaverine and ionophore A23187 on neurulation. *Nature* **261,** 497-499.

Moran, D. J. (1976). A scanning electron microscopic and flame spectrometry study on the role of Ca^{2+} in amphibian neurulation using papaverine inhibition and ionophore induction of morphogenetic movement. *J. Exp. Zool.* **198,** 409-416.

Morize, P., Christiansen, A., E., Costa, M., Parks, S. and Wieschaus, E. (1998). Hyperactivation of the *folded gastrulation* pathway induces specific cell shape changes. *Development* **125,** 589-597.

Morrissette, N., Gold, E. and Aderem, A. (1999). The macrophage-a cell for all seasons. *Trends Cell Biol.* **9**, 199-201.

Morriss-Kay, G. M. (1981). Growth and development of pattern in the cranial neural epithelium of rat embryos during neurulation. *J Embryol. Exp. Morphol.* **65 Supplment,** 225-241.

Myat, M. M. and Andrew, D. J. (2000). Organ shape in the Drosophila salivary gland is controlled by regulated, sequential internalization of the primordia. *Development* **127,** 679-691.

Nardi, J. B. (1981). Induction of invagination in insect epithelium: paradigm for embryonic invagination. *Science* **214,** 564-566.

Oda, H., Tsukita, S. and Takeichi, M. (1998). Dynamic behavior of the cadherin-based cell-cell adhesion system during Drosophila gastrulation. *Dev. Biol.* **203,** 435-450.

Parks, S. and Wieschaus, E. (1991). The Drosophila gastrulation gene *concertina* encodes a G alpha-like protein. *Cell* **64,** 447-458.

Reuter, R., Panganiban, G. E. F., Hoffmann, F. M. and Scott, M. P. (1990). Homeotic genes regulate the spatial expression of putative growth factors in the visceral mesoderm of *Drosophila* embryos. *Development* **110,** 1031-1040.

Seshaiah, P. (2000). Identification and characterization of two genes expressed in the developing Drosophila salivary gland. *Ph.D. Thesis; Johns Hopkins University School of Medicine*, 116-154.

Song, Z. and Steller, H. (1999). Death by design: mechanism and control of apoptosis. *Trends Cell Biol.* **9,** M49-52.

Spooner, B. S. and Wessells, N. K. (1972). An analysis of salivary gland morphogenesis: role of cytoplasmic microfilaments and microtubules. *Dev. Biol.* **27,** 38-54.

Sweeton, D., Parks, S., Costa, M. and Wieschaus, E. (1991). Gastrulation in *Drosophila*: the formation of the ventral furrow and posterior midgut invaginations. *Development* **112,** 775-789.

Tepass, U., Fessler, L. I., Aziz, A. and Hartenstein, V. (1994). Embryonic origin of hemocytes and their relationship to cell death in *Drosophila*. *Development* **120,** 1829-1837.

Weigel, D., Bellen, H. J., Jürgens, G. and Jäckle, H. (1989a). Primordium specific requirement of the homeotic gene *fork head* in the developing gut of the *Drosophila* embryo. *Roux's Arch. Dev. Biol.* **198,** 201-210.

Weigel, D., Jürgens, G., Küttner, F., Seifert, E. and Jäckle, H. (1989b). The homeotic gene *fork head* encodes a nuclear protein and is expressed in the terminal regions of the *Drosophila* embryo. *Cell* **57,** 645-658.

White, K., Grether, M. E., Abrams, J. M., Young, L., Farrell, K. and Steller, H. (1994). Genetic control of programmed cell death in Drosophila. *Science* **264,** 677-683.

Wrenn, J. T. (1971). An analysis of tubular gland morphogenesis in chick oviduct. *Dev. Biol.* **26,** 400-415.

Young, P. E., Pesacreta, T. C. and Kiehart, D. P. (1991). Dynamic changes in the distribution of cytoplasmic myosin during *Drosophila* embryogenesis. *Development* **111,** 1-14.

Young, P. E., Richman, A. M., Ketchum, A. S. and Kiehart, D. P. (1993). Morphogenesis in Drosophila requires nonmuscle myosin heavy chain function. *Genes Dev.* **7,** 29-41.